

ASSESSMENT OF THE THERAPEUTIC EFFICACY OF GALACTOSYLATED CHITOSAN NANOPARTICLES LOADED WITH DOXORUBICIN UNDER THE EFFECT OF ULTRASOUND IRRADIATION IN THE TREATMENT OF HEPATOCELLULAR CARCINOMA IN MICE AND EVALUATION OF THEIR CARDIOTOXICITY

HEBA S. RAMADAN*[#], TAHA I. HEWALA**

*Medical Biophysics Department, Medical Research Institute, Alexandria University, 21561, Egypt,
[#]e-mail: elfarouk22005@yahoo.com

**Radiation Sciences Department, Medical Research Institute, Alexandria University, 21561, Egypt

Abstract. Objective. To evaluate the therapeutic efficacy and cardiotoxicity of galactosylated chitosan nanoparticles containing doxorubicin (DOX-loaded GC-NPs) under the effect of ultrasound irradiation. **Materials and Methods.** DOX-loaded GC-NPs were prepared and characterized before being injected intraperitoneal (i.p.) into mice bearing chemically induced hepatocellular carcinoma (HCC) in the presence and absence of ultrasound irradiation. The other HCC bearing mice were injected i.p. with free DOX in the presence and absence of ultrasound irradiation. For all mice, serum alpha-fetoprotein (AFP) and transforming growth factor- β 1 (TGF β 1), hepatic alanine transaminase (ALT) and cardiac aspartate transaminase (AST), lactate dehydrogenase (LDH) and creatine kinase (CK) activities were determined. **Results.** DOX-loaded GC NPs were having the following criteria: average particle size of 100.4 nm, completely spherical, in the nanoscale with no agglomeration, mean drug loading efficiency (DLE) of 23.26% and mean encapsulation efficiency (EE) of 66.6%. The HCC-bearing mice treated with DOX-loaded GC NPs showed significant decreases in hepatic ALT activity, serum AFP and TGF β 1 levels compared with HCC-bearing mice treated with free DOX which were ameliorated by ultrasound irradiation. Moreover, the HCC-bearing mice treated with DOX-loaded GC-NPs either in the presence or absence of ultrasound irradiation revealed significant declines in the activities of cardiac AST, LDH and CK compared with HCC-bearing mice treated with free DOX and the levels of these cardiotoxicity markers reached their normal values as in the normal control group. **Conclusion.** It could be concluded that treatment of HCC-bearing mice with DOX-loaded GC-NPs combined with ultrasound irradiation was a better therapeutic modality than free DOX with no cardiotoxicity.

Key words: Galactosylated chitosan nanoparticles, doxorubicin, ultrasound irradiation, hepatocellular carcinoma, cardiotoxicity.

Received: May 2016;
in final form July 2016.

INTRODUCTION

Hepatocellular carcinoma is a common disease that represents the 2nd and 6th cancer among males and females in Egypt [35]. Among Egyptians, the incidence of HCC was 12.8% which was 5 to 7 times greater than that in other Middle East Cancer Consortium (MECC) populations. This high rate may be due to the prevalence of hepatitis B and C viruses or to consumption of food contaminated with aflatoxins [20].

Alpha-fetoprotein is a specific tumor marker for diagnosis of HCC. In addition to its use in the diagnosis of hepatocellular carcinoma, the study of serum concentrations of AFP has resulted in significant insights into tumor properties and the process of chemical carcinogenesis [33]. The application of a sensitive radioimmunoassay to AFP reveals that AFP synthesis by the liver is stimulated with remarkable rapidity by extremely low doses of several hepatocarcinogens [14].

Transforming growth factor-beta1 is a potent cytokine synthesized by activated stimulated mesenchymal cells due to chronic liver damage [21]. TGFβ1 is postulated to link chronic injury, cirrhosis, and HCC [4]. It is revealed that TGFβ1 regulates the expression of many genes related to tumor growth [29]. It was found that HCC patients showed over expression of TGFβ1 compared with control subjects which supports the pro-oncogenic function of TGFβ1 in initiating HCC. Although the mechanism is still unknown, TGFβ1 is expected to play an important role in HCC occurrence in cirrhotic patients [5].

Doxorubicin, in the form of doxorubicin hydrochloride, is a cytotoxic anthracycline antibiotic used in the treatment of a wide spectrum of human neoplasms including breast, lung, stomach and liver cancer. The mechanism of its anticancer effect involves its binding to the DNA leading to the inhibition of DNA replication [42]. Due to the side effects of DOX including myelosuppression, cardiotoxicity, the emergence of multidrug resistance and its low specificity against cancer cells, its medical use is limited [39]. The free radicals generated due to the use of DOX initiate cardiotoxicity leading to elevation of cardiotoxicity markers such as lactate dehydrogenase and creatine kinase [49].

Nanotechnology can ameliorate the therapeutic potential of DOX and, at the same time, decrease its undesired effects during cancer treatment. Recently, there are several nanoparticle-based therapeutic systems that revealed low cell toxicity, sustained drug release and molecular targeting. The effective nanoparticle drug delivery system can deliver the drug to cancer cells by two pathways: the first pathway is the passive targeting that makes use of the enhanced permeability and retention effects of tumor blood vessels. The second pathway is the active targeting

in which DOX is allowed to reach cancer cells using ligands or antibodies against selected tumor targets [39].

The binding of galactose to a modified chitosan polymer resulting in the formation of galactosylated chitosan (GC) compound which has a high affinity for binding to its specific asialoglycoprotein receptor (ASGPR) on the hepatocytes membrane. About two millions of ASGPR are found on every hepatocyte [23].

A previous study used GC nanoparticle for gene transfection with high ability to transfer gene into the liver with low cell toxicity [11]. However, the drug delivery efficiency of nanoparticles needs to be improved. Ultrasound targeted delivery enhanced the therapeutic potential of the drug loaded nanoparticles by increasing tissue penetration and cell membrane permeability, although the exact mechanism of action is not well clarified [24].

The present study aimed to assess the therapeutic efficacy of active targeting of GC nanoparticles containing doxorubicin under the effect of ultrasound irradiation and, at the same time, to figure out whether this therapeutic modality can ameliorate the side effects of DOX on cardiac tissues.

MATERIALS AND METHODS

PREPARATION OF DOX-LOADED GC NANOPARTICLES

Galactosylated chitosan was previously prepared by coupling of water-soluble chitosan with the galactose moiety of lactobionic acid (LA) [52]. Then, 1% w/v solution of galactosylated chitosan and doxorubicin hydrochloride (30% w/w DOX: GC Polymer) were added dropwise into 25 mL liquid paraffin containing 5% w/v span 20 as a surfactant and stirred under magnetic stirrer (Newtec.co magnetic stirrer MG model 2004) for 15–20 min. Then, 0.5 mL of 0.5% w/v solution of sodium tripolyphosphate (TPP) was added under magnetic stirring for 5 min. The nanoparticles suspension was gently stirred for 60 minutes at room temperature. The suspension was centrifuged for 60 minutes at 14,000 rpm at 4 °C (HettichR MIKROR 120 Centrifuge) and particles were separated. The particles produced were washed with deionized water then allowed for drying before being subjected to lyophilization [37].

Pellets were suspended in deionized water using ultrasonication (Branson ultrasonic cleaner B-220 50/60 Hz) for 3 min. The colloidal suspension was pre-frozen at –80 °C for 24 h. D-Trehalose 5% was added as cryoprotectant to the

colloidal suspension before the final freeze-drying. Particles were freeze-dried at 50 °C for 12 h by lyophilization, and the particles powder was used for further characterization and application [32].

CHARACTERIZATION OF DOX-LOADED NANOPARTICLES

The size of the prepared particles was determined by Dynamic Light Scattering (DLS) on a Beckman Coulter Particle Size Analyzer (N5 submicron particle size analyzer, Japan). Transmission Electron Microscope (Jeol, JSM-6360LA, Japan) was used to study the shape of the prepared particles [32]. The drug entrapment efficiency and drug loading efficiency of DOX-GC NPs were determined by the method of Hao *et al.* [16] in which DOX-GC NPs solution was ultracentrifuged and the supernatant was withdrawn to determine the concentration of DOX by reading its absorbance at 480 nm using UV-VIS spectrophotometer (Jenway, UK). The drug loading efficiency and entrapment efficiency was calculated as follows:

$$EE = \frac{T - F}{T} \times 100\% \quad (1)$$

$$DLE = \frac{T - L}{W} \times 100\% \quad (2)$$

where T is total DOX concentration in GC nanoparticles, F is free DOX concentration in the supernatant, DLE is drug loading efficiency and W is the weight of DOX-GC NPs.

ANIMAL HANDLING AND CARE

The present study was conducted on 80 Swiss albino mice, 6–8 weeks old, weighing 16–25 g, purchased from animal house at National Cancer Institute, Cairo University. They were housed in the experimental animal unit in the Medical Technology Center, Medical Research Institute, Alexandria University, Egypt. Each ten animals were housed in a plastic cage in a well-ventilated room ($25 \pm \pm 2$ °C). The animals were maintained in a controlled environment under standard conditions of temperature and humidity with an alternating 12 h light/dark cycle with free access to water and food. All animals were fed standard pellet diet. Animals were handled according to the rules and regulations of Medical Research Institute Animal Ethics Committee.

INDUCTION OF HEPATIC TUMOR IN MICE

Mice were fed on 0.06% 4-dimethylaminoazobenzene (DAB) [9] dissolved in paraffin oil at a daily dose of 165 mg/kg body weight per mouse through a fine pipette and water was replaced with 0.05% aqueous solution of phenobarbital (PB) for two months until appearance of liver tumor [3]. Hepatic tumor induction was histopathologically confirmed. One to three mm-thick perpendicularly oriented gross sections were obtained from each excised tumor or control specimens. These sections were immediately fixed in 10% formaldehyde solution for at least 6 hours followed by paraffin embedding. Four μm formalin-fixed, paraffin embedded tissue sections from each case were then routinely stained with H&E stain for histopathologic investigation.

EXPERIMENTAL DESIGN

After one week of acclimatization and before any treatment, the 80 male mice were randomly divided into 2 main groups:

Group I: it included 20 normal mice which were subdivided into two subgroups as follows:

Subgroup IA: it included 10 normal control mice (control subgroup).

Subgroup IB: it included 10 normal control mice that were exposed to ultrasonic waves for 15 min (control + US subgroup).

Group II: it included 60 HCC mice which were further subdivided into six subgroups as follows:

Subgroup II A: it included 10 mice that were administered PBS intraperitoneally (i.p) and served as an untreated group (untreated HCC subgroup).

Subgroup II B: it included 10 mice that were administered PBS intraperitoneally (i.p) and exposed to ultrasonic waves for 15 min (HCC+ US subgroup).

Subgroup II C: it included 10 mice. Each mouse was administered i.p with free DOX at an accumulative dose of 15 mg/kg body weight; divided into three doses, each dose 5 mg/kg, each other day; (HCC+free DOX subgroup).

Subgroup II D: it included 10 mice. Each mouse was administered i.p with free DOX at an accumulative dose of 15 mg/kg body weight; divided into three doses, each dose 5 mg/kg, each other day; and exposed to ultrasonic waves for 15 min after 30 min of DOX administration (HCC+free DOX+US subgroup).

Subgroup II E: it included 10 mice. Each mouse was administered i.p with DOX-loaded GC NPs at an accumulative dose of 15 mg/kg body weight; divided into three doses, each dose 5 mg/kg, each other day; (HCC+ DOX-GCNPs subgroup).

Subgroup II F: it included 10 mice. Each mouse was administered i.p with DOX-loaded GC NPs at an accumulative dose of 15 mg/kg body weight; divided into three doses, each dose 5 mg/kg, each other day; and exposed to ultrasonic waves for 15 min after 30 min of DOX-loaded GC NPs administration (HCC+ DOX-GCNPs+ US subgroup).

ULTRASOUND IRRADIATION

After 30 min of intraperitoneal injection of DOX-loaded GC nanoparticles, animals were exposed for 15 min to ultrasonic irradiation using ultrasonic therapy instrument (Ultrasonic Therapy Model CSL, Shanghai, No.822 factory, China) [31]. The transducer of this instrument is calcium zirconate titanate with frequency of 0.8 MHz at a pulsed mode. The output power is 0.5–3 W and the diameter of beam emitted (BeD) was estimated according to the equation:

$$BeD = 0.2568(D) \times SF \quad (3)$$

where D : transducer diameter and SF : flat surface, normalized focal length of the transducer surface. It was found that for flat surface, $SF = 1$. For the 1 cm diameter flat surface transducer used in the present work, $BeD \approx 0.26$ cm.

The treatment protocol of free and loaded-DOX was administered for one week (3 times for one week only). Within 1–2 h after the final treatment, the animals in each subgroup were anaesthetized and sacrificed, blood samples, liver and cardiac tissues were collected for biochemical analysis. Sera were harvested by blood centrifugation for 15 min at 3500 rpm at 4 °C and stored in aliquots at –80 °C until assayed.

SAMPLE PREPARATION FOR BIOCHEMICAL ANALYSIS

Liver and heart tissue biopsies were excised from animals and blood was removed by perfusing the tissue with a cold phosphate buffered saline (PBS, pH = 7.4, 0.1 M). Tissues were blotted on a filter paper to remove excess buffer. The biopsy was weighed and homogenized in PBS. The whole homogenate was centrifuged at 1600 rpm for 20 min at 5 °C, the supernatant was immediately stored at –20 °C for further use.

ASSESSMENT OF THE THERAPEUTIC EFFICACY OF TREATMENT

For evaluation of the therapeutic efficacy of the treatment, serum levels of alpha fetoprotein (AFP) and transforming growth factor- β 1 (TGF β 1), and hepatic ALT activity were determined quantitatively at the Radiation Sciences Department, Medical Research Institute, Alexandria University, Egypt.

DETERMINATION OF SERUM AFP LEVELS IN THE STUDIED GROUPS

The serum levels of AFP were determined using a ready-to-use ELISA kit (eBioscience, North America) according to the manufacture's protocol. Briefly, 50 μ L diluted sera, standards and quality control were added to their respective microplates wells and incubated for 30 min at 37 °C, and then washed. 50 μ L enzyme conjugate were added to each well except for blank well. Microplate wells were incubated for 30 min at 37 °C, and then washed. 50 μ L substrate A and substrate B were added for each well. Microplate wells were incubated for 15 min at 37 °C. 50 μ L stop solution was added to each well with mixing. Absorbance at 450 nm of each well was measured using a microplate reader. A calibration curve was constructed from which unknown AFP concentrations in samples were interpreted.

DETERMINATION OF SERUM TGF β 1 LEVELS IN THE STUDIED GROUPS

The serum levels of transforming growth factor- β 1 (TGF β 1) were determined using a ready-to-use ELISA kit (eBioscience, North America) according to the manufactures protocol. Briefly, 100 μ L sera, standards and quality control were added to their respective microplates wells. 100 μ L assay buffer were added to the blank well. Plate with 96 wells was incubated at room temperature for 2 h on a rack shaker (600 rpm) and then washed. 100 μ L of biotin-conjugate were added to each well. Plate with 96 wells was incubated at room temperature for 1 hr on a rack shaker (600 rpm) and then washed. 100 μ L streptavidin-horseradish peroxidase (HRP) were added to all wells followed by incubation at room temperature for 30 on a rack shaker (600 rpm) and then washed. 100 μ L of tetramethylbenzidine (TMB) substrate were added to all wells followed by incubation at room temperature for 30 min in dark. 100 μ L of stop solution were added to each well. Absorbance at 450 nm of each well was measured using a microplate reader. A calibration curve was constructed from which unknown TGF β 1 concentrations in samples were interpreted.

DETERMINATION OF HEPATIC ALT ACTIVITIES IN THE STUDIED GROUPS

Hepatic ALT activities were determined using a ready-for-use colorimetric kit (Randox, Germany) according to Reitman's & Frankel's colorimetric method. In brief, ALT catalyzes the conversion of alanine and 2-oxoglutarate to pyruvic acid and glutamic acid. The pyruvic acid is treated with 2, 4-dinitrophenylhydrazine in an alkaline medium to form a highly colored pyruvate

hydrazone. ALT is measured by monitoring the concentration of pyruvate hydrazone which is measured spectrophotometrically at 505 nm.

EVALUATION OF THE POSSIBLE CYTOTOXIC EFFECTS ON CARDIAC TISSUES

The possible cytotoxic effects of treatment on cardiac tissues were evaluated through quantitative determination of cardiac AST, LDH and CK activities.

DETERMINATION OF CARDIAC AST ACTIVITIES IN THE STUDIED GROUPS

Cardiac AST activities were determined using a ready-for-use colorimetric kit (Randox, Germany) according to Reitman's & Frankel's colorimetric method. In brief, AST catalyzes the conversion of L-aspartate and 2-oxoglutarate to oxaloacetate and glutamic acid. Oxaloacetate spontaneously decarboxylates to form pyruvate under the strongly acidic conditions. The pyruvate concentration is determined spectrophotometrically in the form of hydrazone, which is produced by reaction with 2,4-dinitrophenylhydrazine in an alkaline medium. The pyruvate hydrazone absorbs at 505 nm.

DETERMINATION OF CARDIAC LDH ACTIVITIES IN THE STUDIED GROUPS

The cardiac Lactate dehydrogenase (LDH) activity was determined using a ready-to-use colorimetric kit (Abcam, UK) according to the manufacturer's protocol. In this assay, LDH reduces NAD to NADH which then interacts with a specific probe to produce a color which is measured photochemically at 450 nm.

DETERMINATION OF CARDIAC CK ACTIVITIES IN THE STUDIED GROUPS

The cardiac Creatine Kinase (CK) activity was determined using a ready-to-use colorimetric kit (Abcam, UK) according to the manufacturer's protocol. In this assay, creatine kinase converts creatine into phosphocreatine and adenosine diphosphate (ADP). The generated phosphocreatine and ADP react with CK Enzyme Mix to form an intermediate which reduces a colorless probe to a colored product with strong absorbance at 450 nm.

RESULTS

The particle size distribution curve for galactosylated chitosan nanoparticles showed sharp distribution range of nanoparticles with an average particle size of 100.4 nm and only 10% were oversized with baseline error of 3.29% at diffraction angle 11.1° and with polydispersity index (*PI*) of 0.707 (Fig. 1).

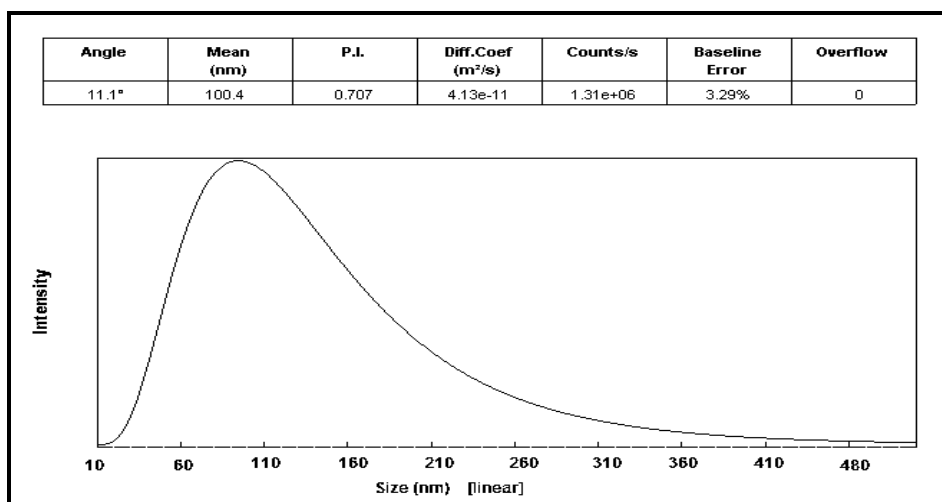


Fig. 1. Particle size distribution curve for prepared DOX-loaded GC nanoparticles.

TEM examination revealed the preparation of galactosylated chitosan nanoparticles which were completely spherical in shape and in the nanoscale with no agglomeration (Fig. 2). The mean drug loading efficacy of the prepared GCs nanoparticles was 23.26% and the mean encapsulation efficacy was 66.6%.

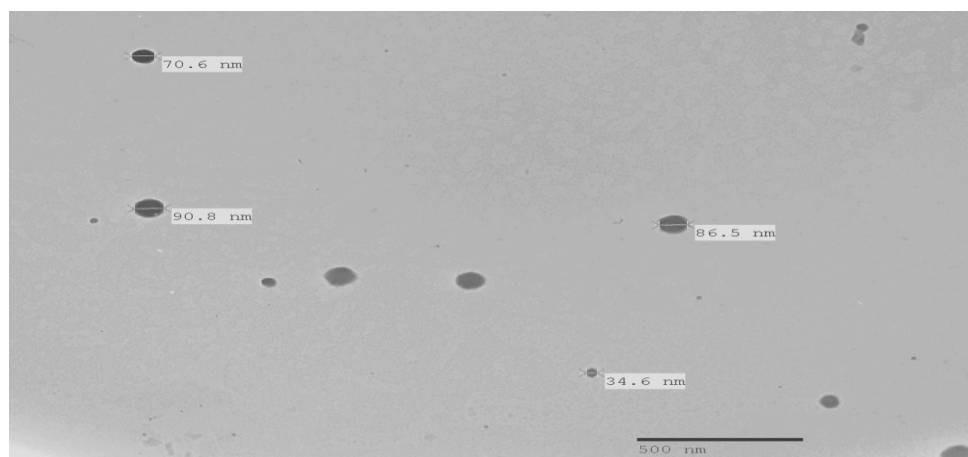


Fig. 2. TEM showing spherical galactosylated chitosan nanoparticles (Mag. 5000 \times , 80 kV).

After 60 days of chronic feeding of DAB and PB, tissue sections of mice livers showed well differentiated HCC as indicated by areas of multinucleated cells and hyperchromated hepatocytes (Fig. 3). Moreover, congested large central vein

with liver tissues which lost their architecture was also observed (Fig. 4) compared with normal control liver tissues (Fig. 5).

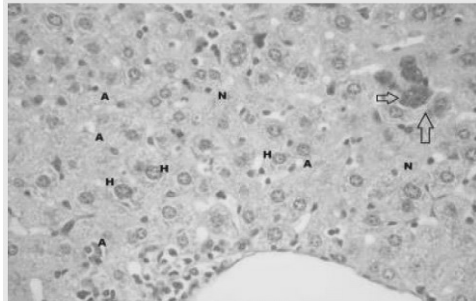


Fig. 3. Paraffin section photograph of mice liver after 60 days of DAB and PB feeding showing areas of multinucleated cells (↑), new angiogenesis formed (A), some necrotic cells (N) and hyperchromated hepatocytes (H). H&E, magnification 4×.

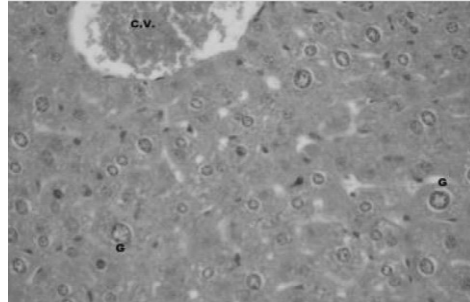


Fig. 4. Paraffin section photograph of mice liver after 60 days of chronic DAB and PB feeding showing congested large central vein (C.V.), the liver tissue lost its architecture, giant cells have large nuclei with the chromatin migrated at nuclear contour (G). H&E, Magnification 4×.

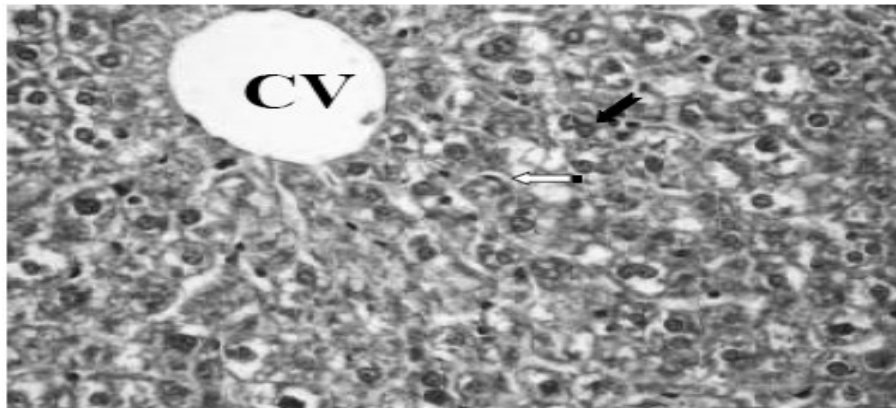


Fig. 5. Paraffin section of control mouse liver showing normal structure, binucleated (→) and central vein (CV). H&E, magnification 4×.

As shown in Table 1, there was no significant difference in the hepatic ALT activity and levels of serum AFP and TGFβ1 between the normal control subgroup and the normal control subgroup exposed to US irradiation ($p = 0.253, 0.110, 0.170$, respectively). Also, there was no significant difference in the hepatic ALT activity and levels of serum AFP and TGFβ1 between the untreated HCC subgroup and the HCC subgroup exposed to US irradiation ($p = 0.610, 0.250, 0.350$, respectively).

The untreated HCC subgroup showed significant elevations in the levels of serum AFP and TGF β 1 and hepatic ALT activity compared with the normal control subgroup ($p = 0.002, 0.006, 0.003$, respectively). The HCC-bearing mice treated with free DOX revealed significant decreases in the levels of serum AFP and TGF β 1 and hepatic ALT activity when compared with untreated HCC-bearing mice ($p = 0.015, 0.025, 0.031$, respectively) but their levels still significantly above their corresponding levels in the normal control mice ($p = 0.023, 0.001, 0.005$, respectively) with no significant effect of ultrasonic wave exposure ($p = 0.081, 0.09, 0.07$, respectively; Table 1). The histopathologic examination of liver tumor tissues showed proliferating lymphocytes around dilated bile duct (B.D.) and congested portal tract (P.T.), increased number of hepatocytes with intranuclear inclusion and eosinophilic cytoplasm and some regenerative hepatocytes (Fig. 6).

The HCC-bearing mice treated with DOX encapsulated into GC nanoparticles showed significant decreases in the levels of serum AFP and TGF β 1 and hepatic ALT activity when compared with the HCC-bearing mice treated with free DOX ($p = 0.043, 0.038, 0.005$; respectively) which were ameliorated by ultrasonic wave exposure in which the levels of the three biomarkers reached remained their normal levels as in the normal control group ($p = 0.151, 0.257, 0.112$; respectively; Table 1). The histopathologic examination of liver tumor tissues taken from the mice of these groups showed an increased number of apoptotic bodies and defined liver cords (Fig. 7).

Table 1

Mean \pm SE of hepatic ALT activities and levels of serum AFP and TGF β 1 in the studied groups

Subgroups	Hepatic ALT (U/g tissues)	Serum AFP (pg/mL)	Serum TGF β 1 (ng/mL)
Control	28.49 \pm 0.79	30.97 \pm 2.23	2.24 \pm 0.11
Control+US	30.21 \pm 0.65	32.03 \pm 1.50	2.13 \pm 0.09
Untreated HCC	186.33 \pm 23.55 ^a	179.34 \pm 12.60 ^a	5.38 \pm 0.38 ^a
HCC+US	182.27 \pm 22.6	175.59 \pm 13.5	4.82 \pm 0.46
HCC+ free DOX	90.85 \pm 7.23 ^{a,b}	85.19 \pm 5.99 ^{a,b}	4.26 \pm 0.12 ^{a,b}
HCC+ free DOX+US	60.6 \pm 2.91 ^{a,b}	76.67 \pm 5.39 ^{a,b}	3.83 \pm 0.27 ^{a,b}
HCC+DOX-GCNPs	78.85 \pm 2.07 ^{a,b,c}	62.77 \pm 4.11 ^{a,b,c}	3.14 \pm 0.11 ^{a,b,c}
HCC+DOX-GCNPs+US	32.68 \pm 1.44 ^{b,c,d}	37.66 \pm 2.65 ^{b,c,d}	2.88 \pm 0.13 ^{b,c,d}

a. Significance was compared with control group. b. Significance was compared with untreated HCC subgroup. c. Significance was compared with HCC+ free DOX subgroup. d. Significance was compared with HCC+DOX-GCNPs subgroup.

As shown in Table 2, the cardiac AST, LDH and CK activities were within the same range in the untreated HCC subgroup and the HCC subgroup exposed to US irradiation ($p = 0.066, 0.084, 0.765$, respectively). There was no significant difference in the activities of cardiac AST, LDH and CK between the normal control mice and untreated HCC-bearing mice ($p = 0.140, 0.199, 0.220$; respectively). The mice bearing HCC and treated with free DOX either in the presence ($p = 0.038, 0.041, 0.04$, respectively) or absence ($p = 0.001, 0.005, 0.003$, respectively) of ultrasonic irradiation showed significant elevation in the activities of cardiac AST, LDH and CK compared with untreated HCC-bearing mice. The mice bearing HCC and treated with DOX encapsulated into GC NPs revealed significant declines in the activities of cardiac AST, LDH and CK compared with HCC-bearing mice treated with free DOX either in the presence ($p = 0.009, 0.02, 0.025$, respectively) or absence ($p = 0.007, 0.001, 0.028$, respectively) of ultrasound waves exposure. At the same time, the activities of cardiac AST, LDH and CK in HCC-bearing mice treated with DOX encapsulated into GC NPs reached their normal values as in the normal control mice either in the presence ($p = 0.072, 0.09, 0.12$, respectively) or absence ($p = 0.093, 0.16, 0.131$, respectively) of ultrasonic irradiation.

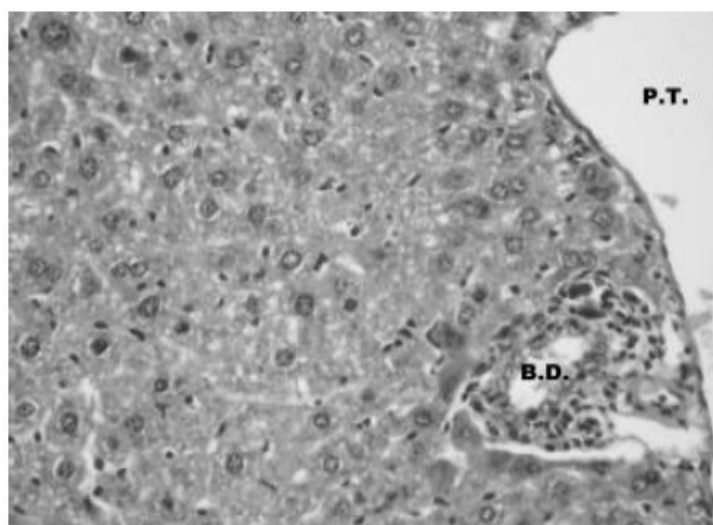


Fig. 6. Paraffin section photograph of mice liver treated with free DOX and exposed to US irradiation showing proliferating lymphocytes around dilated bile duct (B.D.) and congested portal tract (P.T.), increased number of hepatocytes with intranuclear inclusion and eosinophilic cytoplasm, some regenerative hepatocytes (H&E, Mag. $4\times$).

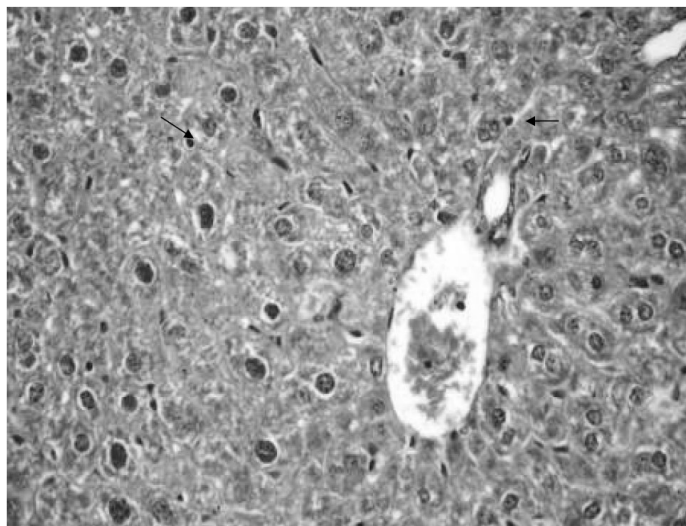


Fig. 7. Paraffin section of mouse liver treated with DOX loaded GC NPs and exposed to US irradiation showing increased apoptotic bodies (→) and defined liver cords (H&E, Mag. 4 ×).

Table 2

Mean± SE activities of cardiac AST, LDH and CK in the studied groups

Subgroups	Cardiac AST (U/g tissue)	Cardiac LDH (U/g tissue)	Cardiac CK (U/mg tissue)
Control	34.19±1.00	436.76±3.78	5.43±2.39
Control+US	35.22±0.8	434.68±2.97	6.01±2.23
Untreated HCC	40.78 ± 3.78	452.31±11.15	15.94±3.11
HCC+US	39.5±3.25	456.50±9.57	14.52±2.98
HCC+ free DOX	223.59±28.27 ^{a,b}	608.39±21.18 ^{a,b}	60.10 ±5.24 ^{a,b}
HCC+ free DOX+US	172.31±11.83 ^{a,b}	591.21±14.53 ^{a,b}	49.06±4.64 ^{a,b}
HCC+DOX-GCNPs	54.63±2.49 ^c	453.68±8.42 ^c	28.02±4.28 ^c
HCC+DOX-GCNPs+US	43.76±3.27 ^c	455.27±7.65 ^c	16.72±2.35 ^c

a: Significance was compared with control group. b: Significance was compared with untreated HCC subgroup. c: Significance was compared with references.

DISCUSSION

Hepatocellular cancer (HCC) is a lethal malignancy with poor prognosis [36]. The stages of HCC development include cirrhosis, adenoma and dysplastic nodule formation [15]. A previous study reported that chronic feeding of the azodye p-dimethylaminoazobenzene (p-DAB) was able to initiate liver cancer [6].

Also, it was found that chronic feeding of phenobarbital (PB) was able to promote liver cancer in human and rodents [8, 38, 48].

In the current study, the chronic feeding of mice with DAB and PB for 60 days has been successfully used to develop liver tumors. Liver carcinogenesis was confirmed histopathologically by the presence of areas of multinucleated cells, formation of new blood vessels (angiogenesis), giant cells having large nuclei with the chromatin migrated at nuclear contour, hyperchromated hepatocytes and the liver tissue lost its architecture. In agreement with our present study, Biswas *et al.* [7] induced hepatocarcinogenesis in mice using DAB and PB and reported that liver nodules appeared after chronic feeding of DAB and PB for 60 days. Also, in Hassan's study [17] HCC induced by 2-nitropropane (2-NP) and N-nitrosodiethylamine (DEN) was confirmed by the loss of hepatic architecture with proliferating streaks and cords of malignant hepatocytes.

It is well documented that AFP determination remains a useful test in the management of patients with HCC [25]. In the current study, hepatic tumor formation was biochemically confirmed by the significant elevation of the serum levels of AFP and TGF β 1 in HCC mice compared with normal control mice. This was in accordance with Baig *et al.* [2] who investigated the diagnostic significance of AFP and concluded that elevated levels of AFP were noted in patients with HCC.

The current therapeutic modalities for HCC include liver transplantation and chemotherapy, with each modality having its limitations [13, 27]. To overcome the non-selectivity of chemotherapy and to minimize its side effects [34], targeted chemotherapy may be the solution as it is a cheap and safe therapeutic modality [19, 28].

Although doxorubicin (DOX) is a chemotherapeutic drug used for cancer treatment, it is not commonly used due to its cardiotoxic effects [46]. Nanoparticles can improve the efficacy of chemotherapeutic drugs by enhancing the entry of drugs into the targeted organ with no effect on surrounding normal tissues eliminating the unwanted effects [51].

Asialoglycoprotein receptor (ASGP-R) is a specific binding site for asialoglycoproteins that is found abundantly on the membrane of hepatocytes [43]. Binding of ligands containing terminal galactose moieties to the ASGP-R results in complex formation which is rapidly internalized by hepatocytes, then the receptor recycled back to the surface of hepatocytes and is reutilized, allowing high binding capacity and efficient uptake of galactosylated ligands by hepatocytes [22].

Chitosan, a modified natural carbohydrate biocompatible polymer, is suitable for mucosal drug delivery [40, 45] with high ability to control the release and targeting of different biomolecules [53]. Galactosylated chitosan (GC) is a galactose ligand, with chitosan modifications on the molecular structure [52]. So, for targeted therapy of HCC, galactosylated chitosan nanoparticles (GCs NPs)

encapsulating DOX were prepared. Our results revealed formulation of spherical GCs NPs with average particle size of 100.4 ± 3.29 nm as revealed by TEM and particle size analyzer, respectively. The size of the nanoparticles in TEM image was smaller than the size measured by DLS, because DLS provides the data for the particles swollen in solution, whereas TEM shows the images of dried nanoparticles. The drug loading efficacy of the prepared GCs nanoparticles was 23.26% and encapsulation efficacy was 66.6%. Our results were approximately in accordance with Wang *et al.* [47] who synthesized norcantharidin-loaded GC nanoparticles (NCTD-GC NPs) with an average particle size of 118.68 ± 3.37 nm, encapsulation efficacy of $57.92 \pm 0.40\%$, and drug loading efficacy of $10.38 \pm 0.06\%$.

For targeted therapy of hepatocellular carcinoma, Zhu *et al.* [53] prepared nanoparticles composed of galactosylated chitosan oligosaccharide and adenosine triphosphate (ATP), with an average diameter of 51.03 ± 3.26 nm, encapsulation efficacy of 88.98%, drug loading efficacy of 26.25% and they reported that these properties were suitable for a drug delivery system.

In the present study, when DOX was encapsulated into GCs-NPs and administered to HCC-bearing mice, the hepatic ALT activity and serum AFP and TGF β 1 levels were significantly decreased compared with their levels in untreated HCC mice, but their levels are still significantly higher than their normal levels. Moreover, Exposure of HCC mice treated with DOX encapsulated into GCs-NPs to ultrasonic irradiation significantly ameliorated the therapeutic effect of GC-NPs as indicated by the significant decrease in the levels of Hepatic ALT, serum AFP and TGF β 1 as the levels of these markers reached their normal values.

Several pathways were proposed for the enhancing effects of ultrasound irradiation on drug-loaded nanoparticles delivery. The first pathway is that ultrasound (US) irradiation induces pores formation on the cell membrane that accelerates the internalization of drug-loaded nanoparticles [44]. The second pathway is that exposure of the cell to ultrasound (US) irradiation generates free radicals that increases the permeability of the cell membranes to drug-loaded nanoparticles [26]. The other pathways postulated that the improved effects of ultrasound irradiation on drug-loaded nanoparticles may be due to increasing endocytosis and activating cell membrane transport [30] or may be due to elevating the local temperature of cell membrane which affects the liquidity of the membrane phospholipid bilayer and enhancing the cell membrane internalization [50, 10].

Rapoport *et al.* [41] were able to treat mice bearing xenograft breast tumors using DOX-loaded polymer nanomicrobubbles under the enhancing effect of US irradiation. Hauff *et al.* [18] were capable of treating rats bearing HCC using

plasmid pU t651MB encapsulated into nanoparticles aided by US irradiation. Yang *et al.* [50] managed to transfect plasmid GFP-loaded chitosan alginate nanoparticles into HeLa and 293T cells under the effect of US irradiation.

In the current study, the HCC-bearing mice treated with free DOX showed significant decreases in the levels of serum AFP and TGF β 1 and hepatic ALT activity when compared with untreated HCC-bearing mice with no significant effect of ultrasound irradiation and the levels of these markers still significantly above their corresponding levels in the normal control mice either in the presence or absence of ultrasound irradiation. At the same time, in the subgroup of HCC mice treated with free DOX, there was significant elevation in the activities of cardiac AST, LDH and CK compared with untreated HCC-bearing and also compared with the normal control mice, which indicated that mice treated with free DOX suffered from severe cardiotoxicity. Our current results confirmed those of Divakaran *et al.* [12] who stated that DOX is a potent chemotherapeutic drug for cancer treatment whose clinical utility is restricted due to its harmful effects on the heart.

Also in the current study, HCC mice treated with DOX encapsulated into GCs-NPs in the presence of US irradiation showed significant decrease in the levels of serum AFP and TGF β 1 and hepatic ALT activity. At the same time, the levels of these markers reached their normal values, with no cardiotoxicity. The absence of cardiotoxicity was indicated by the significant reduction in the activities of cardiac AST, LDH and CK which reached their normal levels as in the normal control mice.

It was mentioned that the toxic effects of DOX on cardiac tissues may be related to induction of oxidative stress that results in peroxidation of membrane lipids, damage of mitochondrial membrane, decreased activity of Na⁺/K⁺ ATPase and myocardial injury. Also, DOX may result in elevated levels of cholesterol, triglycerides, and low density lipoprotein, lactate dehydrogenase (LDH) and creatinine kinase (CK) [1]. From the current study, it could be concluded that DOX encapsulated into GCs-NPs may be a promising therapeutic modality in the treatment of DAB-induced HCC in mice compared with free DOX. DOX encapsulated into GCs-NPs combined with ultrasound irradiation can ameliorate cardiotoxicity induced by the use of free DOX.

Author contribution: Authors are equally contributed to this work.

REFERENCES

1. ASENSIO-LOPEZ, M.C., J. SANCHEZ-MAS, D.A. PASCUAL-FIGAL, C. DE TORRE, M. VALDES, A. LAX, Ferritin heavy chain as main mediator of preventive effect of metformin against mitochondrial damage induced by doxorubicin in cardiomyocytes, *Free Radic. Biol. Med.*, 2013, **67C**, 19–29.

2. BAIG, J.A., J.M. ALAM, S.R. MAHMOOD, M. BAIG, R. SHAHEEN, I. SULTANA, A. WAHEED, Hepatocellular carcinoma and diagnostic significance of α -fetoprotein, *J. Ayub Med. Coll. Abbottabad*, 2009, **21**(1), 72–75.
3. BHATTACHARJEE, N., S. PATHAK, A.R. KHUDA-BUKHSH. Amelioration of carcinogen-induced toxicity in mice by administration of a potentized homeopathic drug, natrium sulphuricum 200, *Evid. Based Comp. Alter. Med.*, 2009, **6**(1), 65–75.
4. BISSELL, D.M., Chronic liver injury, TGF-beta, and cancer, *Exp. Mol. Med.*, 2001, **33**, 179–190.
5. BISSELL, D.M., D. ROULOT, J. GEORGE, Transforming growth factor beta and the liver, *Hepatology*, 2001, **34**, 859–867.
6. BISWAS, S.J., A.R. KHUDA-BUKHSH, Cytotoxic and genotoxic effects of the azo-dye p-dimethylaminoazobenzene in mice: A time-course study, *Mutat. Res.*, 2005, **587**, 1–8.
7. BISWAS, S.J., N. BHATTACHARJEE, A.R. KHUDA-BUKHSH, Efficacy of a plant extract (*Chelidonium majus* L.) in combating induced hepatocarcinogenesis in mice, *Food and Chemical Toxicology*, 2008, **46**, 1474–1487.
8. BISWAS, S.J., S. PATHAK, A.R. KHUDA-BUKHSH, Assessment of the genotoxic and cytotoxic potentials of an anti-epileptic drug, phenobarbital, in mice, *Mutat. Res.*, 2004, **563**, 1–11.
9. BISWAS, S.J., S. PATHAK, N. BHATTACHARJEE, J.K. DAS, A.R. KHUDA-BUKHSH, Efficacy of the potentized homeopathic drug, carnosin 200 fed alone and in combination with another drug, chelidonium 200, in amelioration of p-dimethylaminoazobenzene induced hepatocarcinogenesis in mice, *J. Alter. Compl. Med.*, 2005, **11**, 839–854.
10. CHAPPELL, J.C., J. SONG, C.W. BURKE, A.L. KLIBANOV, R.J. PRICE, Targeted delivery of nanoparticles bearing fibroblast growth factor-2 by ultrasonic microbubble destruction for therapeutic arteriogenesis, *Small*, 2008, **4**, 1769–1777.
11. CHENG, M., J. HAN, Q. LI, B. HE, B. ZHA, J. WU, R. ZHOU, T. YE, W. WANG, H. XU, Y. HOU, Synthesis of galactosylated chitosan/5-fluorouracil nanoparticles and its characteristics, *in vitro* and *in vivo* release studies, *J. Biomed. Mater. Res. B Appl. Biomater.*, 2012, **100**, 2035–2043.
12. DIVAKARAN, S.A., C.K. NAI, Amelioration of doxorubicin induced cardiotoxicity in tumor bearing mice by ferulic acid: a mechanistic study at cellular and biochemical level, *International Journal of Tumor Therapy*, 2012, **1**(2), 6–13.
13. DOYLE, M.B., N. VACHHARAJANI, E. MAYNARD, S. SHENOY, C. ANDERSON, J.R. WELLEN, J.A. LOWELL, W.C. CHAPMAN, Liver transplantation for hepatocellular carcinoma: long-term results suggest excellent outcomes., *J. Am. Coll. Surg.*, 2012, **215**(19), 28–30.
14. FAUSTO, N, Mouse liver tumorigenesis: models, mechanisms, and relevance to human disease. *Semin. Liver Dis.*, 1999, **19**, 243–252.
15. FEITELSON, M.A., B. SUN, N.L. SATIROGLU TUFAN, J. LIU, J. PAN, Z. LIAN, Genetic mechanisms of hepatocarcinogenesis, *Oncogene.*, 2002, **21**, 2593–2604.
16. HAO, H., Q. MA, C. HUANG, F. HE, P. YAO, Preparation, characterization, and *in vivo* evaluation of doxorubicin loaded BSA nanoparticles with folic acid modified dextran surface, *International Journal of Pharmaceutics*, 2013, **444**, 77–84.
17. HASSAN, S.M., Comparative histopathological & immunohistochemical studies between melatonin and grape-seed extract in treating hepatocellular carcinoma, *J. Am. Sci.*, 2012, **8**(12), 132–137.
18. HAUFF, P., S. SEEMANN, R. RESZKA, M. SCHULTZE-MOSGAU, M. REINHARDT, T. BUZASI, T. PLATH, S. ROSEWICZ, M. SCHIRNER, Evaluation of gas-filled microparticles and sonoporation as gene delivery system: feasibility study in rodent tumor models, *Radiology*, 2005, **236**, 572–578.

19. HOSSAIN, D.M., S. BHATTACHARYYA, T. DAS, G. SA, Curcumin: the multi-targeted therapy for cancer regression, *Front. Biosci. (Schol Ed)*, 2012, **4**, 335–355.
20. IBRAHIM, A.S., Liver and intrahepatic bile duct cancer, in: FREEDMAN, L.S., EDWARDS, B.K., RIES, L.A.G., YOUNG, J.L. (eds), *Cancer Incidence in Four Member Countries (Cyprus, Egypt, Israel, and Jordan) of the Middle East Cancer Consortium (MECC) Compared with US SEER*, National Cancer Institute, NIH Pub. No. 06-5873. Bethesda, MD, 2005 Ch 5; pp. 51–60.
21. INAGAKI, Y, I. OKAZAKI, Emerging insights into transforming growth factor beta Smad signal in hepatic fibrogenesis, *Gut.*, 2007, **56**, 284–292.
22. ISHIHARA, T., A. KANO, K. OBARA, M. SAITO, X. CHEN, T.G. PARK, T. AKAIKE, A. MARUYAMA, Nuclear localization and antisense effect of PNA internalized by ASGP-R-mediated endocytosis with protein/DNA conjugates, *Journal of Controlled Release*, 2011, **155**, 34–39.
23. JIANG, H., H. WU, Y.L. XU, J.Z. WANG, Y. ZENG, Preparation of galactosylated chitosan/tripolyphosphate nanoparticles and application as a gene carrier for targeting SMMC7721 cells, *J. Biosci. Bioeng.* 2011, **111**, 719–724.
24. JING, M.A., L.F. DU, M. CHEN, H.H. WANG, L.X. XING, L.F. JING, Y.H. LI, Drug loaded nano-microcapsules delivery system mediated by ultrasound-targeted microbubble destruction: A promising therapy method, *Biomedical Reports*, 2013, **1**, 506–510.
25. JOHNSON, P.J., The role serum alpha-fetoprotein estimation in the diagnosis and management of hepatocellular carcinoma, *Clin. Liver Dis.* 2001, **5**(1), 145–159.
26. JUFFERMANS, L.J., P.A. DIJKMANS, R.J. MUSTERS, C.A. VISSER, O. KAMP, Transient permeabilization of cell membranes by ultrasound-exposed microbubbles is related to formation of hydrogen peroxide, *Am. J. Physiol. Heart Circ. Physiol.*, 2006, **291**, H1595–H1601.
27. LI, S.F., A.M. HAWXBY, R. KANAGALA, H. WRIGHT, A. Sebastian Liver transplantation for hepatocellular carcinoma: indications, bridge therapy and adjuvant therapy, *J. Okla. State Med. Assoc.* 2012, **105**, 12–16.
28. MANCHUN, S., C.R. DASS, P. SRIAMORNSAK, Targeted therapy for cancer using pH-responsive nanocarrier systems, *Life Sci.*, 2012, **90**, 381–387.
29. MASSAGU, E.J., TGF- β in cancer. *Cell*, 2008, **134**, 215–230.
30. MILLER, D.L., R.A. GIES, The interaction of ultrasonic heating and cavitation in vascular bioeffects on mouse intestine, *Ultrasound Med. Biol.* 1998, **24**, 123–128.
31. MOHAMED, M.M., M.A. MOHAMED, N.M. FIKRY, Enhancement of antitumor effects of 5-fluorouracil combined with ultrasound on Ehrlich ascites tumor *in vivo*, *Ultrasound Med. Biol.*, 2003, **29**(11), 1635–1643.
32. NAGARWAL, R.C., P.N. SINGH, S. KANT, P. MAITI, J.K. PANDIT, Chitosan nanoparticles of 5-fluorouracil for ophthalmic delivery: characterization, *in vitro* and *in vivo* study, *Chem. Pharm. Bull.*, 2011, **59**(2), 272–278.
33. NICHOLAS, K., S. GUILLET, E. TOMLINSON, K. HILLAN, B. WRIGHT, G.D. FRANTZ, T.A. PHAM, L. DILLARD-TELM, S.P. TSAI, J.P. STEPHAN, J. STINSON, T. STEWART, D.M. FRENCH, A mouse model of hepatocellular carcinoma, *Am. J. Pathol.*, 2002, **160**(6), 2295–2307.
34. NUSSBAUMER, S., P. BONNABRY, J.L. VEUTHEY, S. FLEURY-SOUVERAIN, Analysis of anticancer drugs: a review, *Talanta*, 2011, **85**, 2265–2289.
35. OMAR, A, G.K. ABOU-ALFA, A. KHAIRY, H. OMAR, Risk factors for developing hepatocellular carcinoma in Egypt, *Chin. Clin. Oncol.*, 2013, **2**(4), 43–45.
36. PARKIN D.M., F. BRAY, J. FERLAY, P. PISANI, Estimating the world cancer burden: Globocan 2000. *Int. J. Cancer.*, 2001, **94**, 153–156.
37. PATEL, K., M. SHRIMANKER, R. DAVE, H. MODI, J. ANAND, S. BHADANI, Preparation and *in vivo* study of doxorubicin loaded chitosan nanoparticles prepared by w/o emulsion method, *International Journal of Current Research*, 2012, **4**(12), 438–440.

38. PATHAK, S, A.R. KHUDA-BUKHSH, Assessment of hepatocellular damage and hematological alterations in mice chronically fed p-dimethyl aminoazobenzene and phenobarbital, *Experimental and Molecular Pathology*, 2007, **83**, 104–111.
39. PRADOS, J., C. MELGUIZO, R. ORTIZ, C. VÉLEZ ,P.J. ALVAREZ, J.L. ARIAS, M. RUÍZ, V. GALLARDO, A. ARANEGA, Doxorubicin-loaded nanoparticles: new advances in breast cancer therapy, *Anticancer Agents Med. Chem.*, 2012, **12**(9), 1058–1070.
40. RAMESAN, R.M., C.P. SHARMA, Modification of chitosan nanoparticles for improved gene delivery, *Nanomedicine*, 2012, **7**, 5–8.
41. RAPOPORT, N., Z. GAO, A. KENNEDY, Multifunctional nanoparticles for combining ultrasonic tumor imaging and targeted chemotherapy, *J. Natl. Cancer Inst.*, 2007, **99**, 1095–1106.
42. REDDY, L.H., R.S.R. MURTHY, Pharmacokinetics and biodistribution studies of doxorubicin loaded poly(butyl cyanoacrylate) nanoparticles synthesized by two different techniques, *Biomed. Papers*, 2000, **148**(2), 161–166.
43. RIGOPOULOU, E.I., D. ROGGENBUCK, D.S. SMYK, C. LIASKOS, M. MYTILINAIU, E. FEIST, K. CONRAD, D.P. BOGDANOS, Asialoglycoprotein receptor (ASGPR) as target autoantigen in liver autoimmunity: lost and found, *Autoimmunity Reviews*, 2012, **12**, 260–269.
44. SCHLICHER, R.K., H. RADHAKRISHNA, T.P. TOLENTINO, R.P. APKRIAN, V. ZARNITSYN, M.R. PRAUSNITZ, Mechanism of intracellular delivery by acoustic cavitation, *Ultrasound Med. Biol.*, 2006, **32**, 915–924.
45. SHI, B., Z. SHEN, H. ZHANG, J. BI, S. DAI, Exploring *N*-imidazolyl-*O*-carboxymethyl chitosan for high performance gene delivery, *Biomacromolecules*, 2012, **13**, 146–153.
46. SINGAL, P.K., N. ILISKOVIC, Doxorubicin-induced cardiomyopathy, *N. Engl. J. Med.*, 1998, **339**, 900–905.
47. WANG, Q., L. ZHANG, W. HU, Z.H. HU, Y.Y. BEI, J.Y. XU, W.J. WANG, X.N. ZHANG, Q. ZHANG, Norcantharidin-associated galactosylated chitosan nanoparticles for hepatocyte-targeted delivery, *Nanomedicine*, 2010, **6**, 371–381.
48. WHITE, S.J., A.E.M. MCLEAN, C. HOWLAND, Anticonvulsant drugs and cancer, A cohort study in patients with severe epilepsy, *Lancet.*, 1979, **ii**, 458–461.
49. XU, M.F., P.L. TANG, Z.M. QIAN, M. ASHRAF. Effects by doxorubicin on the myocardium are mediated by oxygen free radicals, *Life Sci.*, 2001, **68**, 889–901.
50. YANG, S.J., S.M. CHANG, K.C. TSAI, *et al.*, Effect of chitosan-alginate nanoparticles and ultrasound on the efficiency of gene transfection of human cancer cells, *J. Gene Med.*, 2010, **12**, 168–179.
51. ZHANG, Y., J. LI, M. LANG, X. TANG, L. LI, X. SHEN, Folate-functionalized nanoparticles for controlled 5-Fluorouracil delivery, *J. Colloid Interface Sci.*, 2011, **354**, 202–209.
52. ZHOU, X., M. ZHANG, B. YUNG, H. LI, C. ZHOU, L.J. LEE, R.J. LEE. Lactosylated liposomes for targeted delivery of doxorubicin to hepatocellular carcinoma, *Int. J. Nanomedicine*, 2012, **7**, 5465–5474.
53. ZHU, X.L., Y.Z. DU, R.S. YU, P. LIU, D. SHI, Y. CHEN, Y. WANG, F.F. HUANQ, Galactosylated chitosan oligosaccharide nanoparticles for hepatocellular carcinoma cell-targeted delivery of adenosine triphosphate, *Int. J. Mol. Sci.*, 2013, **14**, 15755–15766.

